INTERNATIONAL JOURNAL OF
ENERGY AND ENVIRONMENT

Volume 5, Issue 2, 2014 pp.239-250
Journal homepage: www.IJEE.IEEFoundation.org

Modeling and analysis of DFIG in wind energy conversion system

Omer Elfaki Elbashir, Wang Zezhong, Liu Qihui

School of Electrical and Electronics Engineering, North China Electric Power University, Beinong Road, Changping district, Beijing, china.

Abstract
This paper deals with the modeling, analysis, and simulation of a doubly-fed induction generator (DFIG) driven by a wind turbine. The grid connected wind energy conversion system (WECS) is composed of DFIG and two back to back PWM voltage source converters (VSCs) in the rotor circuit. A machine model is derived in an appropriate dq reference frame. The grid voltage oriented vector control is used for the grid side converter (GSC) in order to maintain a constant DC bus voltage, while the stator voltage orientated vector control is adopted in the rotor side converter (RSC) to control the active and reactive powers.

Keywords: Wind energy conversion system; DFIG; dq vector control.

1. Introduction
Wind energy is one of the most important and promising sources of renewable energy all over the world, mainly because it is considered to be nonpolluting and economically viable. At the same time, there has been a rapid development of related wind turbine technology [1]. A DFIG is based on a wound rotor induction machine (WRIM). The 3-phase rotor windings are supplied with a voltage of controllable amplitude and frequency using an ac to ac converter. Consequently, the speed can be varied while the operating frequency on the stator side remains constant. Depending on the required speed range, the rotor converter rating is usually low compared with the machine rating. Therefore, a DFIG is preferable for variable speed wind turbine applications [2]. The choice of control strategy incorporated can vary depending on the wind turbine generators, but the most popular control scheme for the DFIG of wind turbine generators is a field oriented control (FOC). This control strategy is well established in the field of variable speed drives and when applied to the DFIG control, allows independent control of the electromagnetic torque and stator reactive power [3].
The DFIG using back to back PWM converters for the rotor side control has been well established in wind power system. When used with a wind turbine it offers several advantages over the fixed speed generator systems. These advantages, including speed control and reduced flickers, are primarily achieved by controlling the voltage source converter, with its inherent bi-directional active and reactive powers flow. Among the various technologies available for wind energy conversion systems, the DFIG is one of the preferred solutions because it reduced mechanical stress and optimized power capture due to the variable speed operation. Variable speed operation of electric generators has been proved to be advantages over the fixed speed systems. Three topologies are now widely preferred for the variable

speed operation, conventional asynchronous generators with full rating power converters, permanent magnet synchronous generators (PMSG's) with full rating power converters and the DFIG with partial rating power converters [4, 5]. A wind energy conversion system using DFIG is shown in Figure 1.

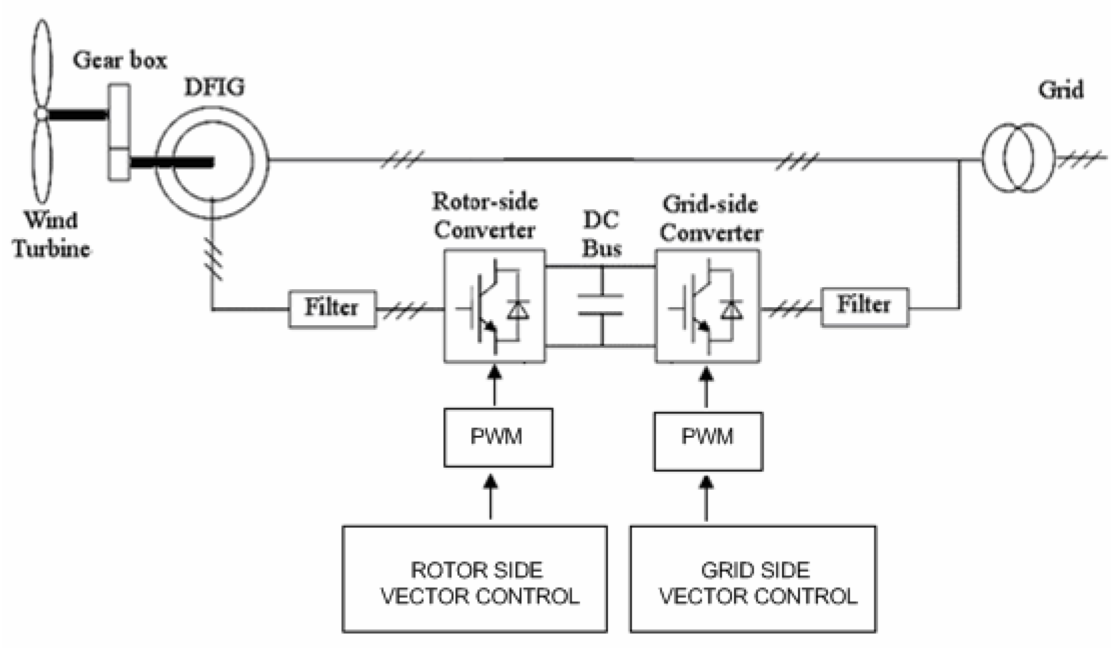

Figure 1. General structure of the wind power generation system with DFIG

In the above system, the stator of the DFIG is directly connected to the grid, while two back to back PWM voltage source converters (VSCs) are inserted between the rotor and the grid to control the rotor and stator output power which is fed to the grid for the variable speed operation [6]. It is possible to control rotor current injection using VSCs to ensure effective operation in both sub and super synchronous modes. Decoupled control of active and reactive powers using the vector control is presented in [7] and current control methods for wind turbines using DFIG are presented in [8]. Both stator and rotor are able to supply the power, but the direction of active power flow through the rotor circuit is dependent on the wind speed and accordingly, the generator speed. Below the synchronous speed, the active power flows from the grid to the rotor side, and the RSC acts as a voltage source inverter while the GSC acts as a rectifier but above the synchronous speed, RSC acts as a rectifier and GSC acts as an inverter. The rotor VSC is controlled to limit the torque pulsation, and the grid VSC is controlled to limit the DC voltage ripple [9]. Two back to back voltage fed current regulated converters are connected to the rotor circuit. The firing pulses are given to the devices (IGBTs) using PWM techniques. The converters are linked to each other by means of DC-link capacitor. The main purpose of the GSC is to control the DC-link voltage and ensures the operation at unity power factor by making the reactive power drawn by the system from the utility grid equal to zero, while the RSC controls the active and reactive powers by controlling the d-q components of the rotor currents i_{dr} and i_{qr}.

2. d-q Model of induction generator

The d-q axis representation of an induction generator is used for simulation, taking flux linkage as a basic variable. It is based on fifth-order two axis representations commonly known as the "Park model" [10]. Here an equivalent 2-phase machine represents 3-phase machine. Where $d^s - q^s$ correspond to the stator direct and quadrature axes, and $d^r - q^r$ correspond to the rotor direct and quadrature axes. A synchronously rotating $d - q$ reference frame is used with the direct $d - axis$ oriented along the stator flux position. In this way, decoupled control between the electrical torque and the rotor excitation current is obtained. The reference frame is rotating with the same speed as the stator voltage. While modeling the DFIG, the generator convention is used, indicating that, the currents are outputs and that power has a negative sign when fed into the grid.

2.1 Axis transformations

The $d-q$ model requires that all the 3-phase variables have to be transformed to the 2-phase synchronously rotating frame [11]. A symmetrical 3-phase induction machine with stationary axes as, bs, cs separated by an angle $2\pi/3$ is considered. Here the 3-phase stationary reference frame's $d^s - q^s$ variables are transformed into the synchronously rotating reference frame $d^e - q^e$. Assume that the $d^s - q^s$ axes are oriented at θ angle. The voltages v_{ds}^s and v_{qs}^s can be resolved into as, bs, cs components in a matrix form as:

$$\begin{bmatrix} v_{as} \\ v_{bs} \\ v_{cs} \end{bmatrix} = \begin{bmatrix} \cos\theta & \sin\theta & 1 \\ \cos(\theta - 120^\circ) & \sin(\theta - 120^\circ) & 1 \\ \cos(\theta + 120^\circ) & \sin(\theta + 120^\circ) & 1 \end{bmatrix} \begin{bmatrix} v_{qs}^s \\ v_{ds}^s \\ v_{0s}^s \end{bmatrix} \tag{1}$$

The corresponding inverse relation is:

$$\begin{bmatrix} v_{qs}^s \\ v_{ds}^s \\ v_{0s}^s \end{bmatrix} = \frac{2}{3} \begin{bmatrix} \cos\theta & \cos(\theta - 120^\circ) & \cos(\theta + 120^\circ) \\ \sin\theta & \sin(\theta - 120^\circ) & \sin(\theta + 120^\circ) \\ 0.5 & 0.5 & 0.5 \end{bmatrix} \begin{bmatrix} v_{as} \\ v_{bs} \\ v_{cs} \end{bmatrix} \tag{2}$$

where v_{os}^s is added as the zero sequence component. Equation (2) represents the transformation of 3-phase quantities into 2-phase $d-q$ quantities. It is more convenient to set $\theta = 0$, so that $q-axis$ is aligned with the $a-axis$ in this case. The sine components of d and q parameters will be replaced with cosine values, and vice versa if $d-axis$ coincides with $a-axis$. If the synchronously rotating $d-q$ axes rotate at a synchronous speed ω_e with respect to $d^s - q^s$ axes, then the voltages on the $d^s - q^s$ axes can be converted into $d-q$ a synchronously rotating frame as:

$$\begin{aligned} v_{qs} &= v_{qs}^s \cos\theta_e - v_{ds}^s \sin\theta_e \\ v_{ds} &= v_{qs}^s \sin\theta_e + v_{ds}^s \cos\theta_e \end{aligned} \tag{3}$$

Resolving the rotating frame parameters into stationary frame:

$$\begin{aligned} v_{qs}^s &= v_{qs} \cos\theta_e + v_{ds} \sin\theta_e \\ v_{ds}^s &= -v_{qs} \sin\theta_e + v_{ds} \cos\theta_e \end{aligned} \tag{4}$$

2.2 DFIG model in synchronous rotating reference frame

For the modeling of DFIG in the synchronously rotating frame, we need to represent the 2-phase stator $(d^s - q^s)$ and rotor $(d^r - q^r)$ circuit variables in a synchronously rotating $(d-q)$ frame as shown below:

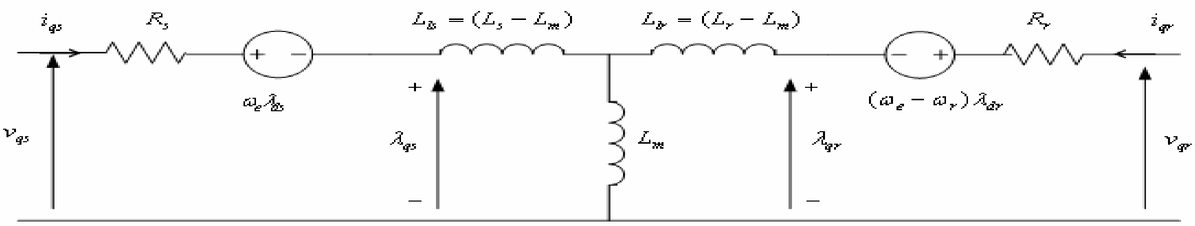

Figure 2. Dynamic d-q equivalent circuit of DFIG (q – axis circuit)

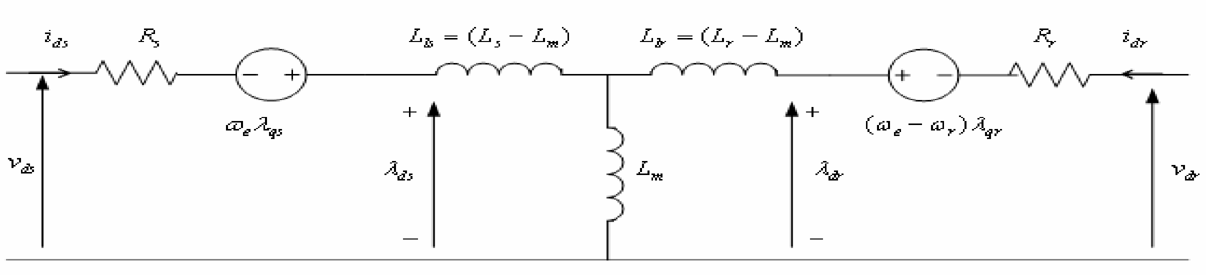

Figure 3. Dynamic d-q equivalent circuit of DFIG (d- axis circuit)

According to Kron's equation, the stator circuit equations are:

$$\begin{aligned} v_{qs}^s &= R_s i_{qs}^s + \frac{d}{dt}\lambda_{qs}^s \\ v_{ds}^s &= R_s i_{ds}^s + \frac{d}{dt}\lambda_{ds}^s \end{aligned} \quad (5)$$

where λ_{qs}^s is the $q-axis$ stator flux linkage, and λ_{ds}^s is the $d-axis$ stator flux linkage respectively. Convert equation (5) to the synchronous rotating frame:

$$\begin{aligned} v_{qs} &= R_s i_{qs} + \frac{d}{dt}\lambda_{qs} + \left(\omega_e \lambda_{ds}\right) \\ v_{ds} &= R_s i_{ds} + \frac{d}{dt}\lambda_{ds} - \left(\omega_e \lambda_{qs}\right) \end{aligned} \quad (6)$$

When the angular speed ω_e is zero the speed of emf due to d and q axis is zero and the equation's changes to stationary form. If the rotor is blocked or not moving, i.e. $\omega_r = 0$, the machine rotor equations can be written in a similar way as the stator equations:

$$\begin{aligned} v_{qr} &= R_r i_{qr} + \frac{d}{dt}\lambda_{qr} + \left(\omega_e \lambda_{dr}\right) \\ v_{dr} &= R_r i_{dr} + \frac{d}{dt}\lambda_{dr} - \left(\omega_e \lambda_{qr}\right) \end{aligned} \quad (7)$$

Let the rotor rotate at an angular speed ω_r, then the $d-q$ axes fixed on the rotor fictitiously will move at a relative speed $(\omega_e - \omega_r)$ to the synchronously rotating frame. The $d-q$ frame rotor equations can be written by replacing $(\omega_e - \omega_r)$ in the place of ω_e as:

$$\begin{aligned} v_{qr} &= R_r i_{qr} + \frac{d}{dt}\lambda_{qr} + \left(\omega_e - \omega_r\right)\lambda_{dr} \\ v_{dr} &= R_r i_{dr} + \frac{d}{dt}\lambda_{dr} - \left(\omega_e - \omega_r\right)\lambda_{qr} \end{aligned} \quad (8)$$

$$\lambda_{qs} = L_{ls} i_{qs} + L_m (i_{qs} + i_{qr}) = L_s i_{qs} + L_m i_{qr} \quad (9)$$

$$\lambda_{ds} = L_{ls} i_{ds} + L_m (i_{ds} + i_{dr}) = L_s i_{ds} + L_m i_{dr} \quad (10)$$

$$\lambda_{qr} = L_{lr} i_{qr} + L_m (i_{qs} + i_{qr}) = L_r i_{qr} + L_m i_{qs} \tag{11}$$

$$\lambda_{dr} = L_{lr} i_{dr} + L_m (i_{ds} + i_{dr}) = L_r i_{dr} + L_m i_{ds} \tag{12}$$

The torque expression can be written in terms of flux linkages and currents as:

$$T_e = \frac{3}{2}\frac{P}{2}(\lambda_{dr} i_{qr} - \lambda_{qr} i_{dr}) \tag{13}$$

3. Control algorithm

Figures 4 and 5 shows the DFIG based WECS with the vector control. The rotor currents are used to control the stator active and reactive powers. The RSC controls the DFIG, while the GSC function is to maintain the DC link voltage constant. The vector control on DFIG is implemented in the two following steps.

3.1 GSC Control

The adopted vector control strategy must fulfill the two main objectives of the grid side converter 1. Regulate DC bus voltage 2. Control reactive power exchanged bidirectional between the rotor of the machine and the grid. Thus, by aligning the grid voltage vector with synchronous frame direct axis, its indirect axis component becomes null $(v_q = 0)$. The active and reactive powers are controlled independently using the vector control strategy. Since the amplitude of supply voltage is constant, the active and reactive powers are controlled by means of i_d and i_q respectively.

$$\begin{aligned} P_s &= \tfrac{3}{2}(v_d i_d + v_q i_q) = \tfrac{3}{2} v_d i_d, (v_q = 0) \\ Q_s &= \tfrac{3}{2}(v_q i_d - v_d i_q) = -\tfrac{3}{2} v_d i_q, (v_q = 0) \end{aligned} \tag{14}$$

where i_d, i_q and v_d are grid current and voltage respectively, as $(v_q = 0)$. Based on the sign of a non-zero slip ratio s, a part of DFIG's generated active power is interchanged with the grid through the rotor, which can deliver or absorb grid's power in super or sub-synchronous modes, respectively. Equation (14), states that active power and consequently, DC bus voltage can be controlled via i_d, whereas i_q can control reactive power flow in the grid. This strategy is depicted in Figure 5. The control signals for the grid converters are:

$$\begin{aligned} v_d^* &= \left(K_{p1} + \frac{K_{i1}}{s}\right)\left[i_d^* - i_d\right] \\ v_q^* &= \left(K_{p1} + \frac{K_{i1}}{s}\right)\left[i_q^* - i_q\right] \end{aligned} \tag{15}$$

where K_p is the proportional gain of the controller, and K_i is the integral gain of the controller. The angular position of the grid voltage is detected using a phase locked loop (PLL), which has good quality in terms of stability and of transient response [12]. This locked angle will be used to transform system variables to the $d-q$ reference frame. The DC bus voltage is maintained constant via the outer voltage PI controller which processes the error between the reference and measured DC bus voltage and yields i_d^*, while i_q^* is set to zero to compensate for reactive power at the grid side. The GSC provides needed magnetizing energy through the rotor for the DFIG. Finally, the measured grid currents (i_d, i_q) and reference currents (i_d^*, i_q^*) are compared then processed by inner current PI controllers, in order to generate appropriate signals for the GSC.

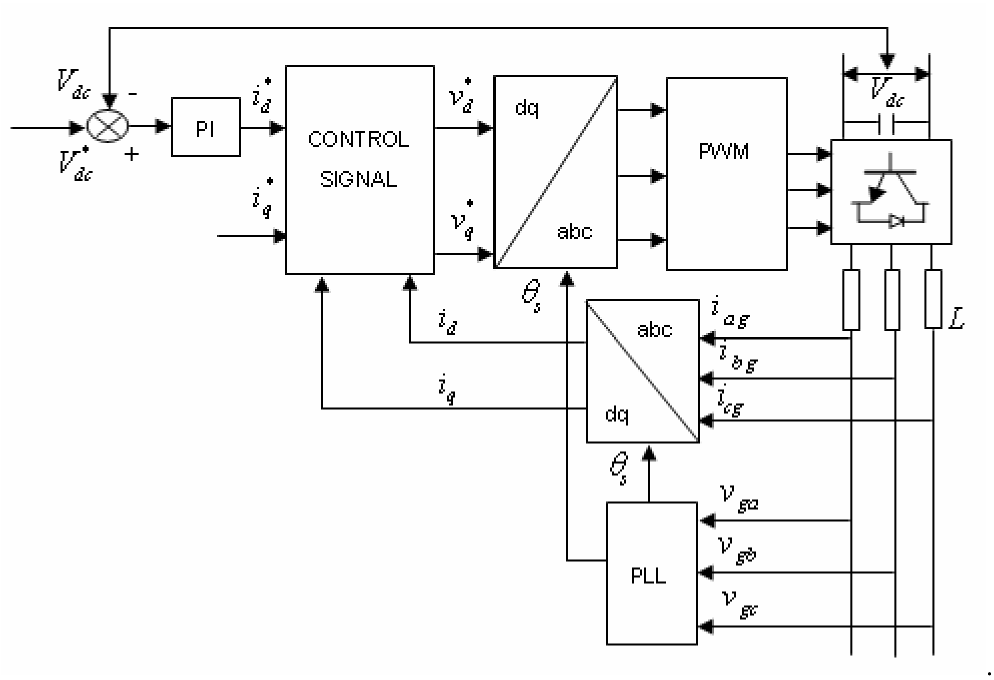

Figure 4. Vector control structure for GSC

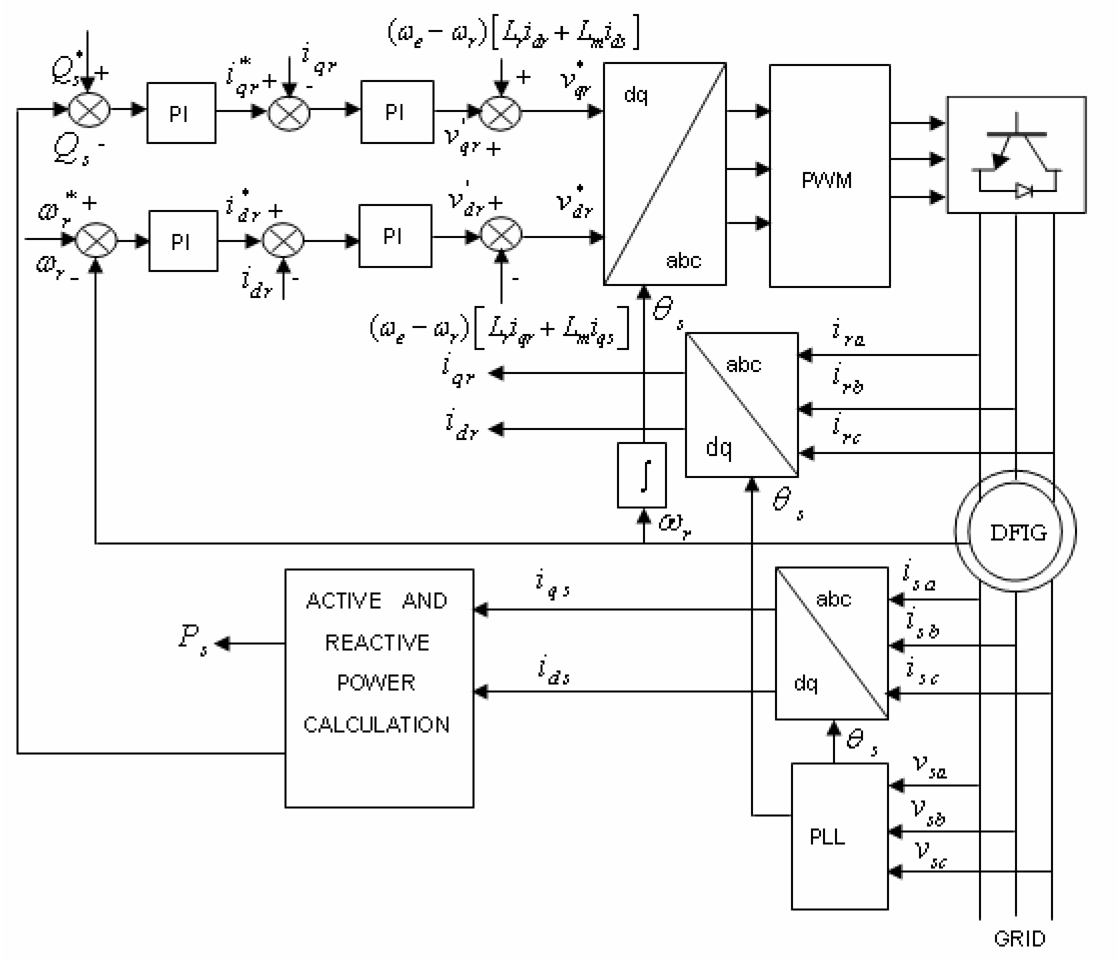

Figure 5. Vector control structure for RSC

3.2 RSC control

The main purpose of the RSC is to maintain the rotor speed constant irrespective of the wind speed and also the control strategy has been implemented to control the active power and reactive powers flow of the machine using the rotor current components. The active power flow is controlled through i_{dr} and the reactive power flow is controlled through i_{qr}. To ensure unit power factor operation like GSC, the reactive power demand is also set to zero here. The standard voltage oriented vector control strategy is used for the RSC to implement control action. Here the real axis of the stator voltage is chosen as the d-axis. Since the stator is connected to the utility grid and the influence of stator resistance is small, the stator magnetizing current i_m can be considered as constant. Under voltage orientation, the relationship between the torque and the $d-q$ axis voltages, currents and fluxes can be written with neglecting of leakage inductances. To maximize the turbine output power, DFIG must be controlled through the control of i_{dr} and i_{qr}. To simplify the control and calculate i_{dr}^*, the stator flux component λ_{ds} is set to zero.

$$\begin{aligned} &\lambda_{ds} = 0 \\ &\lambda_{qs} = (L_{ls} + L_m)i_{qs} + L_m i_{qr} = L_m i_m \end{aligned} \tag{16}$$

The equations of rotor fluxes are:

$$\begin{aligned} &\lambda_{qr} = \frac{L_m}{L_s}\lambda_{qs} + \sigma L_r i_{qr} = \frac{L_m^2}{L_s} i_m + \sigma L_r i_{qr} \\ &\lambda_{dr} = \frac{L_m}{L_s}\lambda_{ds} + \sigma L_r i_{dr} = \sigma L_r i_{dr} \end{aligned} \tag{17}$$

where $\sigma = 1 - \frac{L_m^2}{L_s L_r}$

By substituting the values of λ_{dr} and λ_{qr} from equation (17) in equation (8), the rotor voltages are:

$$\begin{aligned} &v_{dr} = R_r i_{dr} + \sigma L_r \frac{d}{dt} i_{dr} - (\omega_e - \omega_r)\sigma L_r i_{qr} \\ &v_{qr} = R_r i_{qr} + \sigma L_r \frac{d}{dt} i_{qr} + (\omega_e - \omega_r)\sigma L_r i_{dr} \end{aligned} \tag{18}$$

The reference value v_{dr}^* and v_{qr}^* can be found from equation (18) as:

$$\begin{aligned} &v_{dr}^* = v_{dr}' - (\omega_e - \omega_r)[L_r i_{qr} + L_m i_{qs}] \\ &v_{qr}^* = v_{qr}' + (\omega_e - \omega_r)[L_r i_{dr} + L_m i_{ds}] \end{aligned} \tag{19}$$

where v_{dr}' and v_{qr}' are found from the current errors processing through standard PI controllers. The electromagnetic torque can be expressed as:

$$T_e = \frac{3}{2} P \frac{L_m}{L_s} \lambda_{qs} i_{dr} \tag{20}$$

The reference current i_{dr}^* can be found either from the reference torque or from the speed errors through standard PI controllers. Similarly i_{qr}^* can be found from the reactive power errors. The value of i_{dr}^* can be found using equation (20):

$$i_{dr}^* = \frac{T_e^* L_s}{\lambda_{qs} L_m} \tag{21}$$

ISSN 2076-2895 (Print), ISSN 2076-2909 (Online)

4. Results and discussion

A 10hp induction machine whose is specifications are given in Table 1 is simulated using MATLAB/SIMULINK environment. The performance of the DFIG system is analyzed under grid voltage fluctuations. The main objective of this Work is to study the performance analysis of the DFIG for a wind turbine application both during steady-state operation and transient operation. The voltage fluctuations are made by lowering and raising the voltage values in the utility grid intentionally for simulation keeping in view of different grid disturbances (voltage sag).

Table 1. Rating and specifications of DFIG

Rated Power	10 hp
Stator Voltage	415 V
Frequency	60 Hz
Rs (Stator Resistance)	1.1 Ω
Rr (Rotor Resistance)	0.91 Ω
Ls (Stator Inductance)	0.321 H
Lm (Magnitizing Inductance)	0.08 H
Lr (Rotor Inductance)	0.09 H
Poles	6
Rated Speed	1100 rpm
Dc Link Voltage	850 V
Switching Frequency of 1 GBTs	3 kHz

4.1 Simulation under balance grid

DFIG characteristic's waveforms under steady-state conditions are shown in Figure 6. It is observed that, the active and reactive powers supplied by the utility grid are decoupled and DC link voltage is maintained constant due to the control strategy made in the GSC.

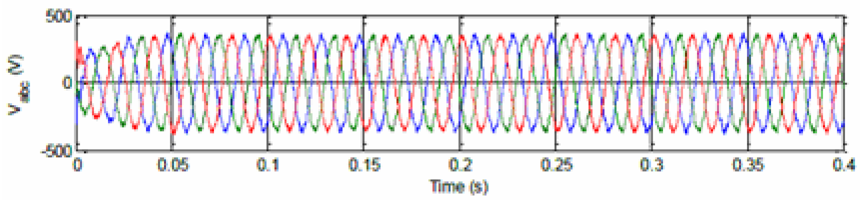

(a) Stator voltage

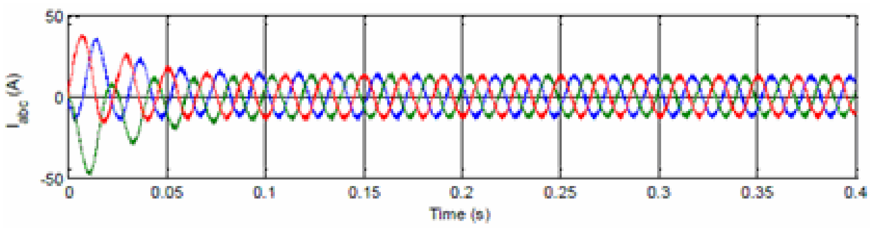

(b) Stator current

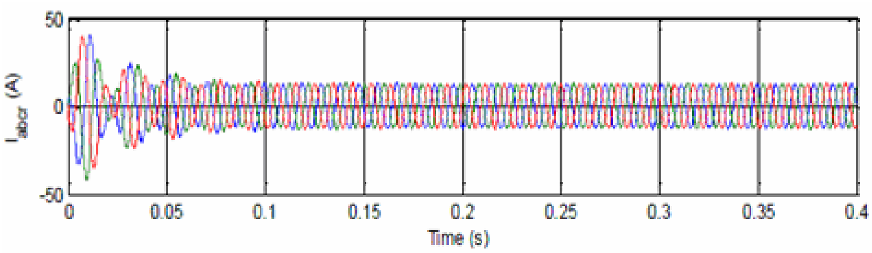

(c) Rotor current

Figure 6. (Continued)

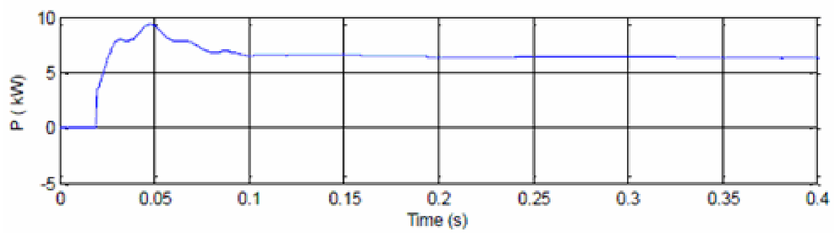

(d) Active power

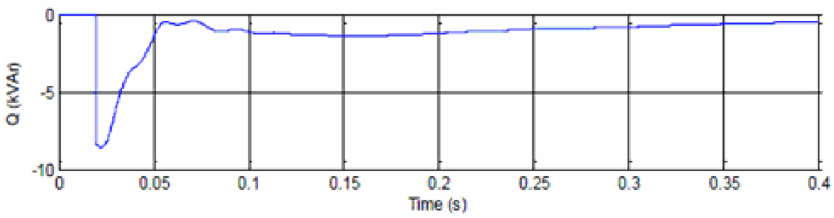

(e) Reactive power

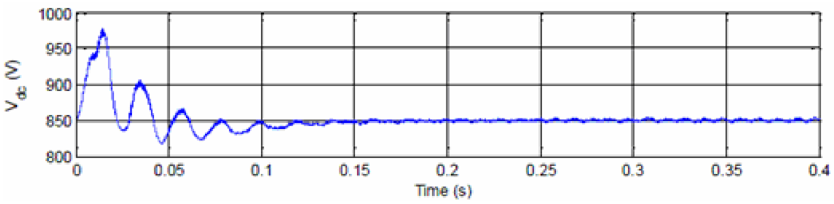

(f) DC link voltage

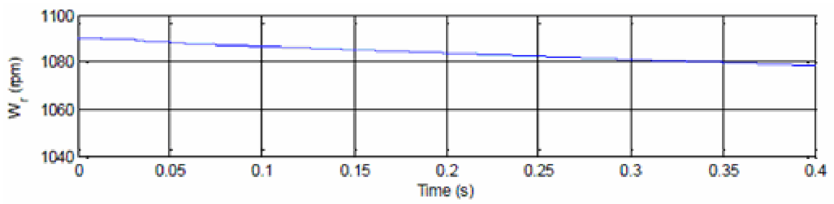

(g) Rotor speed

Figure 6. Simulation results of the grid under balance condition

4.2 Simulation under voltage sag

The simulation results under the voltage sag are shown in Figure 7. The DFIG system produces active power of 7 KW, which corresponds to maximum mechanical turbine output minus electrical losses in the generator. When the grid voltage changes suddenly from its rated value, i.e. 415V the stator current as well as rotor current increases and the active power P suddenly oscillates, and then it settles to its rated value. The reference reactive power is set at 0KVAr but when voltage decreases the reactive power suddenly increases, and then it settles to 0KVAr as the control strategy made in the RSC. The DC link voltage is set at 850V by the GSC at the time of voltage sag oscillates and finally settles to its set value. The rotor speed is also maintained constant to its rated (1080rpm) while the wind speed is kept constant at 10m/s. The rotor output is same as the converter output.

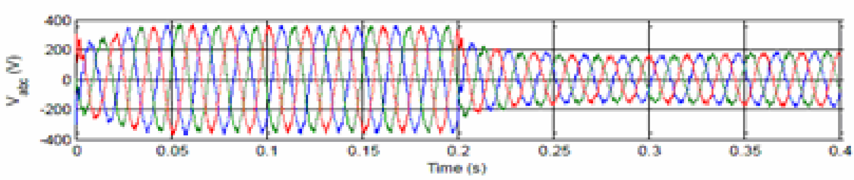

(a) Stator voltage

Figure 7. (Continued)

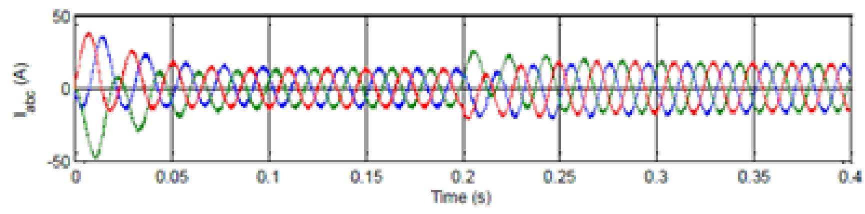

(b) Stator current

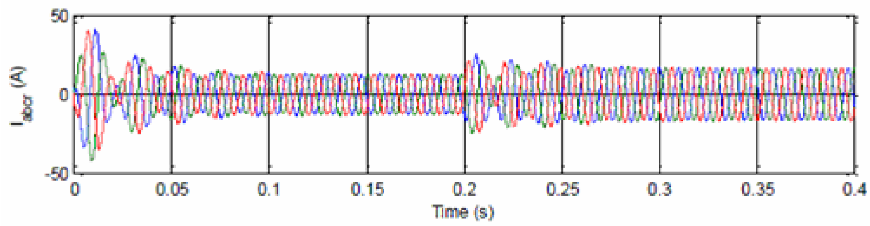

(c) Rotor current

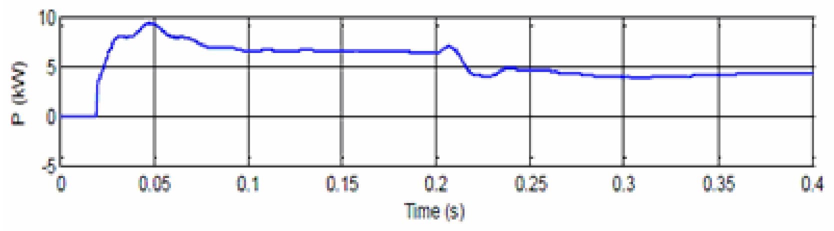

(d) Active power

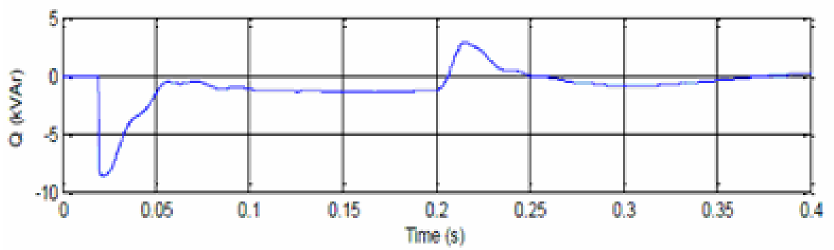

(e) Reactive power

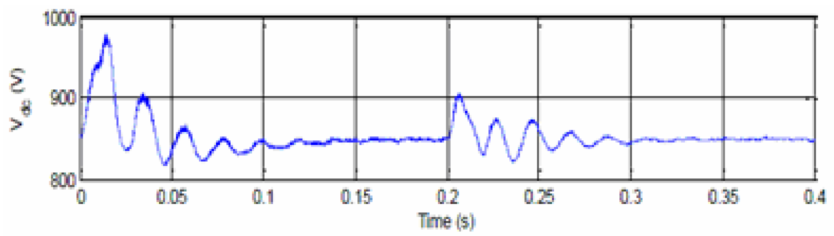

(f) DC link voltage

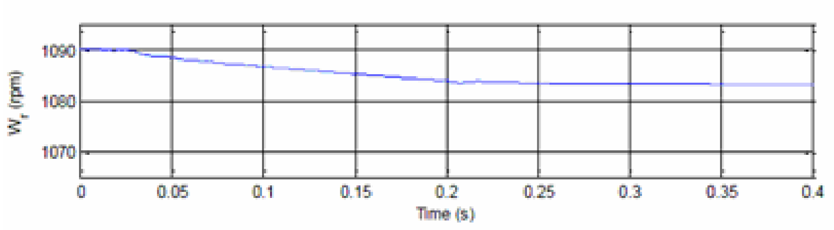

(g) Rotor speed

Figure 7. Simulation results of the grid under voltage sag

5. Conclusion

The main objective of this Work is to study the performance analysis of the DFIG for a wind turbine application both during steady-state operation and transient operation. The modeling, control and simulation of DFIG coupled with a wind turbine has been carried out. The grid connected WECS is composed of DFIG and two back to back PWM voltage source converters in the rotor circuit. The grid voltage oriented vector control is used for the GSC in order to maintain a constant DC bus voltage, while the stator voltage orientated vector control is adopted in the RSC to control the active and reactive powers. The DFIG system is simulated using MATLAB/SIMULINK environment. It is concluded that, the traditional voltage control technique which is used on both GSC as well as the RSC to analyze the performance of the DFIG system under grid voltage fluctuations is suitable under sudden change in grid voltage.

Appendix

Derivation of equation (17)

$$\lambda_{qs} = L_s i_{qs} + L_m i_{qr} \quad (1A)$$

$$\lambda_{qr} = L_r i_{qr} + L_m i_{qs} \quad (2A)$$

Multiply equation (1A) with L_m , and equation (2A) with L_s , we get:

$$L_m \lambda_{qs} = L_m L_s i_{qs} + L_m^2 i_{qr} \quad (1A)$$

$$L_s \lambda_{qr} = L_s L_r i_{qr} + L_s L_m i_{qs} \quad (2A)$$

Substract equation (2A) from equation (1A), we get:

$$L_m \lambda_{qs} - L_s \lambda_{qr} = L_m^2 i_{qr} - L_s L_r i_{qr}$$

$$L_s \lambda_{qr} = L_m \lambda_{qs} + L_s L_r i_{qr} - L_m^2 i_{qr}$$

Divide the equation by L_s

$$\frac{L_s}{L_s} \lambda_{qr} = \frac{L_m}{L_s} \lambda_{qs} + \frac{L_s L_r}{L_s} i_{qr} - \frac{L_m^2}{L_s} i_{qr}$$

$$\lambda_{qr} = \frac{L_m}{L_s} \lambda_{qs} + L_r i_{qr} - \frac{L_m^2}{L_s} i_{qr}$$

$$\lambda_{qr} = \frac{L_m}{L_s} \lambda_{qs} + L_r \left(1 - \frac{L_m^2}{L_r L_s} \right) i_{qr}$$

$$\lambda_{qr} = \frac{L_m}{L_s} \lambda_{qs} + \sigma L_r i_{qr} = \sigma L_r i_{qr}$$

$$because \ \lambda_{qs} = L_m i_m \ and \ i_m \ assumed \ to \ be \ cons\tan t$$

where $\sigma = 1 - \frac{L_m^2}{L_r L_s}$

Similarly

$$\lambda_{dr} = \frac{L_m}{L_s} \lambda_{ds} + \sigma L_r i_{dr} = \sigma L_r i_{dr}$$

$$because \ \lambda_{ds} \ assumed \ to \ be \ zero$$

References

[1] A. Tapia, G. Tapia, J. X. Ostolaza, and J. R. Saenz. Modeling and control of a wind turbine driven doubly-fed induction generator. IEEE Trans. Energy Conv., vol. 18, no. 2, pp. 149-204, June 2003.

[2] Y. Liao, L. Ran, G. A. Putrus, and K. S. Smith. Evaluation of the effects of rotor harmonics in a doubly-fed induction generator with harmonic induced speed ripple. IEEE Trans. Energy Conv., vol. 18, no. 4, pp. 508-515, Dec. 2003.

[3] A. Mullane and M. O'Malley. The inertial response of induction machine-based wind turbines. IEEE Trans. Power Syst., vol. 20, no. 3, pp. 1496-1503, Aug. 2005.

[4] S.S Murthy, Bhim Singh, P.K.Goel and S.K.Tiwari. A Comparative study of fixed speed and variable speed wind energy conversion systems feeding the grid. in Proc. of Int. Conf. on Power Electronics and Drive Systems (PEDS '07), pp. 736-743, 2007.

[5] X.G.Wu, J.B.Ekanayake,andN.Jenkins. Comparison of fixed speed and doubly-fed induction wind turbines during power system disturbances. IEE Proc.-Generation, Transmission and Distribution, vol. 150, no. 3, pp. 343-352, May 2003.

[6] L. Xu and Y. Wang. Dynamic Modeling and Control of DFIG-Based Wind Turbines Under unbalanced Network Conditions. IEEE Trans. Power Systems,vol. 22, no.1, pp.314-323, Feb. 2007.

[7] R. Pena, J. C.Clare, and G.M.Asher. Doubly-fed induction generator using back-to-back PWM converters and its application to variable speed wind energy generation. Proc. Inst. Elect. Eng., Elect. Power Appl., vol.143, no. 3, pp. 231–241, May 1996.

[8] A. Petersson, L.Harnefors, and T. Thiringer. Evaluation of current control methods for wind turbines using doubly-fed induction machines.IEEE Trans. Power Electron., vol. 20, no.1, pp.227–235, 2005.

[9] Z. Yi, P. Bauer, J. A. Ferreira, and J. Pierik. Operation of grid connected DFIG under unbalanced grid voltage condition. IEEE Trans. on Energy Conversion,vol. 24, no. 1, pp. 240-246, March 2009.

[10] G.R.Slemon. Modelling induction machines for electric drives. IEEE Transaction on Industry Application, vol.25, no.6, pp 1126-1131, Nov 1989.

[11] S. Muller, M. Deicke and Rik W. De Doncker. Doubly-fed induction generator systems for wind turbines. IEEE Industry Applications Magazine, May-June, 2002.

[12] S. Rahmani, K. Al-Haddad, and F. Fnaiech. A new control technique based on the instantaneous active current applied to shunt hybrid power filters. in IEEE 34th Annual Power Electronics Specialist Conference, PESC '03, vol.2, pp. 808-813, 2003.

Omer Elfaki Elbashir received his B.Sc degree in Electrical Engineering from sudan University of Science and technology, sudan, in 1999, and his M.sc from Kararry University, sudan 2004. Since 1999, he has been with Kararry University, where he is currently lecturer in the School of Electrical and Electronic Engineering. His current research interest include Electrical Machines, Wind Power Generation and Power System Analysis and Control. Now he started his Ph.D. research in the School of Electrical and Electronic Engineering in North China Electric Power University, China.

Wang Zezhong received the B.Sc., M.Sc. and Ph.D. degrees in Electrical Engineering from Tsinghua University, Beijing, China, in 1983, 1986 and 1989 respectively. Currently, He is a Professor and a Doctor Supervisor at the School of Electrical and Electronic Engineering of North China Electric Power University. His research interests include Numerical Analysis of Complex Electromagnetic Field in Electrical Engineering EMC in Power System, Modern Electromagnetic Measurement. He is one of experts entitled to the Government Special Allowance (GSA) of China. Mr. Wang is a Commissioner of the National Ministry of Education Electrical Engineering and Automation Major Teaching Committee and Senior Member of the Chinese Society for Electrical Engineering.

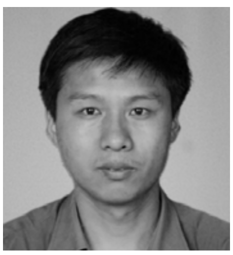

Liu Qihui receive the B.Sc. degree in Mechatronic Engineering from Jinan University, Jinan, China, in 1997, and the M.Sc. degree in Power System and its Automation from Shandong University, Jinan, China, in 2000, and Ph.D. degree in Electrical Engineering from Zhejiang University, Hangzhou, China, in 2005. Since 2005, he has been with North China Electric Power University, where he is currently vice professor in the School of Electrical and Electronic Engineering. His current research interest include wind power generation and integration, distributed generation, and power system analysis and control.

